A Journal of the Gesellschaft Deutscher Chemiker

Angewandte International Edition GDCh Chemie

www.angewandte.org

Accepted Article

Title: Conversion of Methane to Methanol and Ethanol over Nickel Oxide on Ceria-Zirconia Catalysts in a Single Reactor

Authors: Chukwuemeka Okolie, Yasmeen F. Belhseine, Yimeng Lyu, Matthew M. Yung, Mark H. Engelhard, Libor Kovarik, Eli Stavitski, and Carsten Sievers

To be cited as: *Angew. Chem. Int. Ed.* 10.1002/anie.201704704
Angew. Chem. 10.1002/ange.201704704

Link to VoR: http://dx.doi.org/10.1002/anie.201704704
http://dx.doi.org/10.1002/ange.201704704

WILEY-VCH

10.1002/anie.201704704

WILEY-VCH

Conversion of Methane to Methanol and Ethanol over Nickel Oxide on Ceria-Zirconia Catalysts in a Single Reactor

Chukwuemeka Okolie,[a] Yasmeen F. Belhseine,[a] Yimeng Lyu,[a] Matthew M. Yung,[b] Mark H. Engelhard,[c] Libor Kovarik,[c] Eli Stavitski,[d] and Carsten Sievers*[a]

Abstract: Conversion of methane into alcohols under moderate reaction conditions is a promising technology for converting stranded methane reserves into liquids that can be transported in pipelines and upgraded to value-added chemicals. We demonstrate that a catalyst consisting of small nickel oxide clusters supported on ceria-zirconia (NiO/CZ) can convert methane to methanol and ethanol in a single, steady-state process at 723 K using O_2 as an abundantly available oxidant. The presence of steam is required to obtain alcohols rather than CO_2 as the product of catalytic combustion. The unusual activity of this catalyst is attributed to the synergy between the small Lewis acidic NiO clusters and the redox-active CZ support, which also stabilizes the small NiO clusters.

The availability of methane from conventional and unconventional reserves has revolutionized the world's energy mix in recent years (*1*). In conventional processes, methane is reformed into syngas (*2*), which can be used for methanol synthesis (*3*) or be converted to higher hydrocarbons by Fischer-Tropsch synthesis (*4*). Unfortunately, these processes are only economical on large scales, and reforming requires high temperatures (typically > 1100 K). Since transporting gas over long distances is economically challenging, many natural gas reserves are "stranded", and methane is often flared on site rather than used in a productive way. In addition to the loss of a valuable resource, this practice results in greenhouse gas emissions (*5*). Catalytic processes that could enable conversion of methane to liquid products in a single reactor have enormous potential to enable more effective use of stranded gas reserves. This situation has led to intense interest in converting methane to value-added chemicals and fuels (*6-12*).

The conventional route for methanol production uses $Cu/ZnO/Al_2O_3$, ZnO/Cr_2O_3 or similar catalysts at 30-350 bar (*3, 13*). The reaction occurs by sequential hydrogenation of CO or CO_2. Synthesis of ethanol and higher alcohols was reported over Rh, Mo, and modified Fischer–Tropsch or methanol synthesis catalysts and typically also requires elevated pressure (*14*). The proposed routes for C-C bond formation include methanol and CO homologation and CO insertion into metal carbon bonds. Ethanol formation from methanol and syngas was also reported over Cu/SiO_2 catalysts at atmospheric pressure (*15*).

An interesting route for methane activation that might avoid the economy of scale of established routes is direct partial oxidation into oxygenates like methanol, formic acid and formaldehyde or methanol precursors such as methyl bisulphate (*6*). In nature, bacterial methanotrophs convert methane to methanol with metalloenzymes, such as methane monooxygenases (*16*). Soluble monooxygenase contains a carboxylate bridged diiron center, whereas a dicopper cluster has been proposed as the active site of particulate monooxygenase (*17*). While monooxygenases enable an interesting path for methane conversion, they only have limited potential for large scale industrial processes. Inspired by methane monooxygenases, supported phthalocyanine complexes of Fe, Cu, and Co have been investigated (*18-20*). In other studies, methane was converted to methanol over small metal oxide clusters in zeolites, such as bis(μ-oxo) dicopper complexes in Cu/ZSM-5 (*10, 21-26*). However, prohibitively expensive oxidants like tert-butyl hydroperoxide (*18*), H_2O_2 (*10*), or N_2O (*27*) had to be used in many of these studies to generate reactive oxygen species. In other studies, the "catalyst" was reactivated by calcination before it was able to undergo the next turnover (*24, 28*). Thus, the reaction did not occur in a conventional catalytic cycle, in which all elementary reactions occur under the same conditions.

Methane can also be activated at rather mild temperatures (373 – 423 K) by strong Lewis acid sites that are formed when alumina is calcined at high temperature (*29, 30*). However, in many cases, the methyl groups remained on the surface rather than engaging in catalytic turnovers. Nevertheless, this illustrates the potential of Lewis acid sites as parts of bifunctional catalysts.

In this study, we developed a catalyst that is capable of converting methane to alcohols at steady state and moderate temperatures in a single reactor. Steam was necessary to release the alcoholic products, and O_2 acted as an oxidant. This catalyst combines Lewis acid sites with a redox-active ceria-zirconia (CZ) support to enable catalytic turnovers. Additionally, coupling and/or methanol homologation reactions occur, to form ethanol, which is more valuable than methanol.

The CZ support with a molar CeO_2:ZrO_2 ratio of 83:17 was obtained by coprecipitation following a procedure published before (*31, 32*). Al_2O_3, CoO_x, FeO_x, PdO, and NiO clusters on CZ were prepared by dry impregnation of nitrate precursors. The loading was 2 wt.% (on a metal basis) in all cases. The desired Lewis acidic metal oxide clusters were obtained by calcination at 723 K. NiO/SiO_2 with the same Ni loading and NiO/CZ with 5 wt.% Ni were prepared as reference samples.

The concentration of acid sites on each catalyst was determined by pyridine adsorption followed by FTIR spectroscopy. Only the characteristic band of pyridine on Lewis acid sites (LAS) (1445 cm^{-1}) was observed, while none of the spectra contained the characteristic peak of pyridinium ions on Brønsted acid sites (1540 cm^{-1}) (Figure S1). Pure CZ had a low concentration of LAS (2.9 $\mu mol.g^{-1}$), whereas significantly higher values of 80±4 $\mu mol.g^{-1}$ were measured for the samples with additional metal oxide clusters except for Al_2O_3/CZ (Figure S1b). This analysis shows that 26% of the Ni atoms in 2 wt.% NiO/CZ are involved in forming a Lewis acid site (Table S1).

[a] C. Okolie, Y. F. Belhseine, Y. Lyu, Dr. C. Sievers
School of Chemical & Biomolecular Engineering
Georgia Institute of Technology
311 Ferst Drive NW, Atlanta, GA, 30332, United States
Email: carsten.sievers@chbe.gatech.edu
[b] Dr. M. M. Yung
National Renewable Energy Laboratory
15013 Denver West Parkway Golden, CO, 80401, United States
[c] Dr. L. Kovarik, Dr. M.H. Engelhard
Environmental Molecular Sciences Laboratory
Pacific Northwest National Lab
3335 Innovation Blvd., Richland, WA, 99354, United States
[d] Dr. E. Stavitski
National Synchrotron Light Source II
Brookhaven National Laboratory
Upton, NY, 11973, United States

Supporting information for this article is given via a link at the end of the document

The ability of the Lewis acidic catalysts to activate methane was probed by in-situ IR spectroscopy. All samples were activated in vacuum at 723 K. After 1 h of exposure to 530 mbar of methane at 323 K and evacuation for 1 min, CZ only retained a small amount of physisorbed methane as indicated by a small peak at 3014 cm^{-1} (Figure S4a). At temperatures between 373 and 523 K, no stable surface species were observed. This shows that CZ does not have sufficient Lewis acidity for methane activation. On catalysts with additional metal oxide clusters, peaks corresponding to asymmetric and symmetric CH_3 stretching modes were observed around 2957 and 2875 cm^{-1}, respectively, starting at 373 – 423 K (Figure 1 and S4b-g). The intensity of the peaks varied between catalysts with different supported metal oxide clusters, but they were observed for all the samples used in this study. In agreement with previous work on methane activation on γ-Al_2O_3 (*30*), we conclude that methane is activated and that surface methyl or methoxy groups are formed. In case of NiO/CZ and FeO_x/CZ, additional bands were observed around 2921 and 2851 cm^{-1} (Figure 1 and Figure S4e). These peaks are attributed to asymmetric and symmetric CH_2 stretching modes, respectively (*33*). The presence of these bands indicates that surface methyl groups are coupled to longer alkyl or alkoxy chains. Methane activation was also studied on NiO/SiO_2 to probe the role of the CZ support in the activation and coupling of methane. Only the peaks of methyl groups were observed, but no CH_2 groups were formed. This shows that CZ plays a direct or indirect role in enabling the formation of alkyl chains with more than one carbon atom.

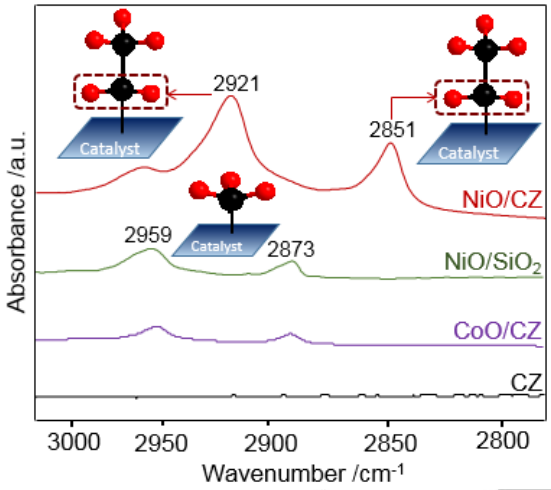

Figure 1. Difference IR spectra of products from CH_4 on selected catalysts at 473 K.

Based on these results, we hypothesized that CZ stabilizes very small, well-dispersed NiO or FeO_x clusters that are capable of activating and coupling methane at low temperatures. Previous reports showed that similar non-metallic Pt and Au species can be stabilized by pure ceria and that these species are highly active as part of water-gas-shift catalysts (*34*). To verify our hypothesis, EDX maps and X-ray diffractograms of NiO/CZ, NiO/SiO_2, and were obtained. The EDX maps of NiO/CZ with 2 wt.% Ni showed the presence of well-dispersed Ni on the entire surface of the CZ support (Figure 2a and S8). The exact size distribution of the Ni clusters cannot be quantified by EDX mapping due to the detectability-stability limits. Nevertheless, it can be concluded that they should be present as NiO clusters below ~2-3 nm in size. In addition to the well dispersed NiO, several larger particles (up to 10 nm) were also occasionally observed. In contrast, the EDX map of NiO/SiO_2 only revealed Ni in the form of larger particles of 10 – 25 nm (Figure 2b). An increase of the Ni loading on CZ to 5 wt.% also resulted in the formation of larger NiO clusters (Figure 2c). In agreement with these results, the X-ray diffractogram of NiO/CZ only contained peaks corresponding to CZ, whereas diffractions of NiO crystallites were observed for NiO/SiO_2 (Figure S3). This shows that the concentration of crystalline particles in 2 wt.% NiO/CZ is below the detection limit for XRD. It is suggested that the high dispersion of NiO on CZ is one prerequisite for the unique activity of these species. In addition, CZ could alter the net charge of the supported NiO clusters or provide interfacial active sites.

Further insight into the synergy between the NiO clusters and the CZ support was obtained by probing the oxidation state of Ni and Ce with in-situ XANES experiments (Figure 3). When NiO/CZ was exposed to a flow of 4% methane in helium at 723 K, the Ce L3-edge shifted to lower energy over the course of 4 h (Figure 3a), indicating reduction of the CZ support. After 4 h, no further shift of the Ce L3-edge could be observed. The final edge position and the line shape with two maxima, which is typical for Ce 4+, indicated that the majority of Ce atom remained in an oxidation state of 4+ with a small contribution from Ce 3+ (*35, 36*). The relatively low white line intensity is attributed to strong Ce fluorescence absorption by ceria matrix. Complementary XPS experiments showed that 49% of the Ce atoms within 3 nm from the surface were reduced to Ce 3+ upon exposure to CH_4 for 4 h at 723 K (Figure S13). Thus, it is suggested that the reduction of CZ at 723 K is mostly limited to surface sites, whereas the bulk essentially remains oxidized (*31, 36*).

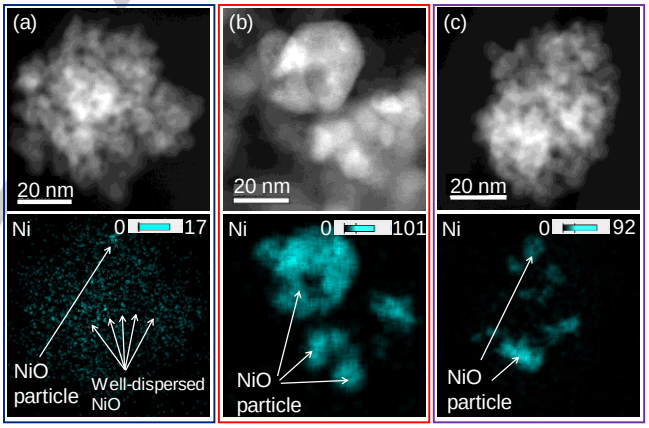

Figure 2. HAADF images and corresponding EDX maps of Ni for (a) 2 wt.% NiO/CZ (b) 2 wt.% NiO/SiO_2 (c) 5 wt.% NiO/CZ. The scales in the Ni EDX maps correspond to the integrated signal from the ionization peak of Ni(K).

The spectrum at the Ni K-edge did not change in the first 4 h while the reduction of CZ was proceeding (Figure 3b). However, a reduction of the white line intensity and a shift of the edge to higher energy occurred within 30 minutes once the reduction of Ce stopped. This shows that NiO clusters are readily converted to metallic Ni when they are present on a reduced CZ surface. Together, the changes of the Ce L3-edge and Ni K-edge indicate that CZ can act as an oxygen reservoir that can supply a certain amount of oxygen to NiO clusters to keep them in the oxidized state. Importantly, CZ has been reported to efficiently activate oxygen even at room temperature via a so-called multiple exchange mechanism (*37*). The combined abilities of activating oxygen and transferring activated oxygen species to

the supported particles, such as the NiO clusters in this study, make CZ an effective component of bifunctional oxidation catalysts (*38, 39*).

In addition to studying the redox behavior of NiO/CZ, we used in-situ XANES to probe the interaction of steam with the supported NiO clusters, since in previous studies the formation of metal hydroxides prevented selective oxidation of methane over CuO_x and FeO_x clusters in steady state (*24, 28*). No changes were observed at the Ni K-edge when NiO/CZ was exposed to steam at 723 K for 4 h (Figure 3c) indicating that the NiO clusters are not converted into hydroxides under these conditions. The derivative of the spectrum provides even clearer evidence for the absence of hydroxyl species (Figure S15). While the white line of the $Ni(OH)_2$ standard showed two distinct maxima, this feature was not observed for the NiO standard or the NiO/CZ catalyst after exposure to steam at 723 K. Thus, it is safe to conclude that NiO clusters are stable in this environment.

Based on the observation of higher alkyl or alkoxy chains on NiO/CZ (Figure 1) and the characterization of this material, we hypothesized that methanol and higher alcohols can be formed over these catalysts. It was shown that steam can hydrolyze surface methoxy species to form methanol (*26*). However, this elementary reaction needs to be coupled with a selective oxidation step to make the process thermodynamically feasible (see SI). Thus, the conversion of methane over 2 wt.% NiO/CZ was studied in a packed bed reactor at 723 K with a feed steam-to-carbon ratio of 1.0, an O_2 to carbon ratio of 0.2, and a balance of nitrogen (Figure 4). The initial methane conversion was 18%. It declined to 15% over the first 3 h on stream, but no further changes were observed after that. If one assumed that every Ni atom of the catalyst constitutes an active site, the conversion of 15% would correspond to a turnover frequency of 50 h^{-1}. Methanol, ethanol, and CO_2 were observed as the main carbon containing products along with hydrogen. The ethanol and methanol yields reached 3.7% and 2.9% on a C atom basis, respectively. This corresponds to a cumulative alcohol selectivity of up to 43%, and an ethanol selectivity of 24% on a C atom basis. The formation of methanol and ethanol was confirmed by NMR spectroscopy (Figures S24a and S25) and MS (Figure S24b). The production of methanol and ethanol throughout the reaction remained almost constant. No products with three or more carbon atoms were observed under the conditions applied here. The formation of H_2 and CO_2 can be attributed to oxy-reforming or a sequence of steam reforming and the water-gas-shift reaction, but oxidation of other surface species could also contribute to the formation of CO_2.

In the initial stage of the reaction, 2.6% of the carbon atoms entering the reactor remained unaccounted for in the product stream and 1.5% were converted to aromatics (Figure 4). Within 5 h, the fractions of unaccounted carbon and aromatics decreased to 0.23% and 0.14%, respectively, and remained at approximately this level for the remaining 3 h of the reaction. Previous reports indicated that coking is typical for Ni particles that have a certain minimum size (*40, 41*). Thus, it is suggested that carbonaceous deposits are formed on the few large NiO clusters (Figure 2a). Some aromatic precursors of these deposits are desorbed instead of being permanently deposited. Once the larger particles are covered, the formation of deposits and aromatics almost ceases. In contrast, the well-dispersed NiO clusters remain accessible and active. Combustion analysis of the spent catalyst indicated the presence of 2.9 wt.% of combustible deposits.

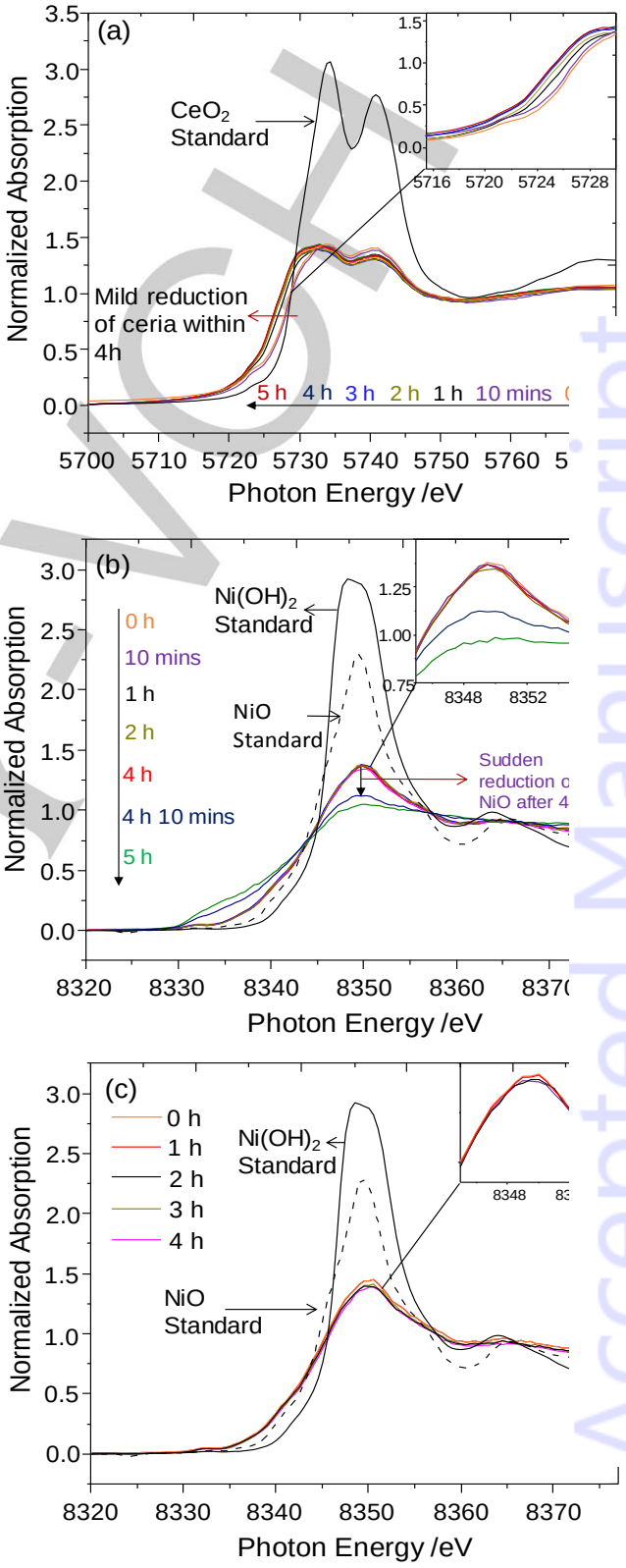

Figure 3. In-situ XANES spectra: (a) Ce L_3-edge during reaction of CH_4 over NiO/CZ at 723 K (b) Ni K-edge during reaction of CH_4 over NiO/CZ at 723 K (c) Ni K-edge during exposure to H_2O at 723 K.

Further evidence for this scenario was obtained when methane was converted under identical conditions over 2 wt.% NiO/SiO_2 and 5 wt.% NiO/CZ, which contained larger NiO particles. Over 2 wt.% NiO/SiO_2, the initial conversion was 15%, but the catalysts deactivated completely over the course of 6 h (Figure S23a). The amount of deposited carbon on the spent catalyst as determined by CHN analysis was 5.8 wt.%, which is significantly higher compared to 2 wt.% NiO/CZ. Only CO and CO_2 were observed as carbon-based products over this catalyst, which demonstrates further that the synergy between NiO and CZ plays a critical role in the production of alcohols. The initial conversion over 5 wt.% NiO/CZ was 23%, but it declined to 13% within 5 h (Figure S22a), and the cumulative alcohol selectivity was only around 30%. These observation show that 5 wt.% NiO/CZ contains fewer small NiO clusters that are active for sustained production of alcohol than 2 wt.% NiO/CZ.

To illustrate the function of steam, 2 wt.% NiO/CZ was used in a reaction with a feed that only contained methane and O_2 in N_2 (Figure S17b). The conversion dropped from 17% to 14% over the first 3 h on stream and remained constant for the rest of the experiment. CO_2 was the only carbon containing product detected. This shows that steam is necessary to obtain alcohols, whereas the combustion of methane dominates in the absence of steam in the feed. With a feed containing only methane, steam and nitrogen, the initial methane conversion was 2% and some alcohols were formed (Figure S17a). However, the catalytic activity ceased within about 4 h, which correspond to the time at which the reduction of Ce stopped during the in-situ XANES experiment under similar conditions.

The observations described above show that NiO clusters can activate methane, similar to the one in previous reports of methane activation on other types of Lewis acidic sites (*29, 30*). In the case of sufficiently large clusters, carbonaceous deposits are formed, and the clusters are deactivated. The CZ support appears to stabilize NiO clusters that are sufficiently small to avoid this deactivation path. In the presence of steam, the surface species can be hydrolyzed and desorbed as alcohols. Based on the in-situ XANES results (Figure 3a and 3b) and well-documented activity of CZ for activating O_2 (*37*), it is suggested that the active oxygen species required for the selective oxidation reaction originate on CZ. However, the exact origin of O atoms in the products will be the subject of future studies. A reference experiment showed that methanol formation over NiO/CZ is also possible from syngas and steam (Figure S18b), but CO was not completely converted.

The strong peaks of alkyl or alkoxy groups with two or more carbon atoms in in-situ IR spectra (Figures 1 and S5) seems to point at a reaction path involving coupling of surface alkyl or alkoxy species. In a reference experiment, ethanol was formed from a mixture of methanol and syngas at the same temperature and pressure (Figure S19). This indicates that homologation might be an alternative reaction path (*14*), but the observation of residual CO in this experiments (as opposed to the absence of CO in the product stream from methane conversion) indicates that homologation is less likely to be the dominant reaction path.

In summary, the present results show that the unique synergy between small NiO clusters and redox-active CZ results in a catalyst that can convert methane to methanol and ethanol in a single reactor. To the best of our knowledge, this is the first report of a single-reactor conversion of methane to ethanol. Unlike in studies of many other materials based on supported metal oxide clusters, all parts of the catalytic cycle occur at the same temperature with a turnover frequency of at least 50 h^{-1}.

Acknowledgements

The work was performed with funds from the Petroleum Research Fund of the American Chemical Society (grant number: 53873) and the U.S. Department of Energy (DOE) Office of Basic Energy Science under Contract No. DE-SC0016486. The XAS data was obtained at beamline 9-BM of the Advanced Photon Source, a U.S. Department of Energy (DOE) Office of Science User Facility operated for the DOE Office of Science by Argonne National Laboratory under Contract No. DE-AC02-06CH11357. EDX mapping and XPS was performed using EMSL a DOE Office Science User Facility sponsored by the Office of Biological and Environmental Research. The Renewable Bioproducts Institute at the Georgia Institute of Technology is thanked for the use of its facilities. We thank Michael Buchanan, Leah Filardi, Sankar Nair, Evgeny Pidko, Andrew J. Medford, and Johannes A. Lercher for experimental support and fruitful discussions.

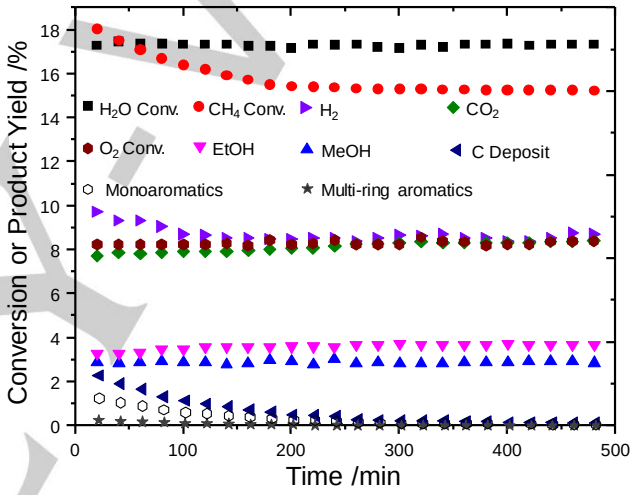

Figure 4. Conversion of methane and O_2 and yields of products formed during reactions of methane, steam and oxygen in a packed bed reactor setup at 723 K and 1 atm over 2 wt.% NiO/CZ. Yields of carbon-containing products are calculated on a carbon atom basis. A space velocity of 3000 h^{-1} of reactant gas diluted in nitrogen was used. Other experimental conditions are detailed in the SI.

Keywords: C-H activation • Heterogeneous catalysis • Lewis acids • Methane • Nickel

1. J. Deutch, *Foreign Aff.* **2011,** *90*, 82-93.
2. J. R. Rostrup-Nielsen, J. Sehested, J. K. Norskov, *Adv. Catal.,* **2002,** *47*, 65-139.
3. P.L. Spath, D.C. Dayton, *Preliminary Screening - Technical and Economic Assessment of Synthesis Gas to Fuels and Chemicals with Emphasis on the Potential for Biomass-Derived Syngas* (NREL, Golden, CO 2003).
4. B. Jager, R. Espinoza, *Catal. Today* **1995,** *23*, 17-28.
5. *Inventory of US greenhouse gas emissions and sinks: 1990-2009* (EPA 430-R-11-005, U.S. Environmental Protection Agency, Washington, D.C., U.S.A., 2011).
6. C. Hammond, S. Conrad, I. Hermans, *ChemSusChem* **2012,** *5*, 1668-1686.
7. X. G. Guo, G. Z. Fang, G. Li, H. Ma, H. J. Fan, L. Yu, C. Ma, X. Wu, D. H. Deng, M. M. Wei, D. L. Tan, R. Si, S. Zhang, J. Q. Li, L. T. Sun, Z. C. Tang, X. L. Pan, X. H. Bao, *Science* **2014,** *344*, 616-619.
8. J. Gao, Y. Zheng, J. Jehng, Y. Tang, I. E. Wachs, S. G. Podkolzin, *Science* **2015,** *348*, 686-690.

9. A. T. Ashcroft, A. K. Cheetham, J. S. Foord, M. L. H. Green, C. P. Grey, A. J. Murrell, P. D. F. Vernon, *Nature* **1990,** *344*, 319-321.
10. C. Hammond, M. M. Forde, M. H. Ab Rahim, A. Thetford, Q. He, R. L. Jenkins, N. Dimitratos, J. A. Lopez-Sanchez, N. F. Dummer, D. M. Murphy, A. F. Carley, S. H. Taylor, D. J. Willock, E. E. Stangland, J. Kang, H. Hagen, C. J. Kiely, G. J. Hutchings, *Angew. Chem.-Int. Ed.* **2012,** *51,* 5129-5133; *Angew. Chem.* **2012,** *124,* 5219-5223.
11. M. Lin, A. Sen, *Nature* **1994,** *368*, 613-615.
12. R. A. Periana, J. D. Taube, S. Gamble, H. Taube, T. Satoh, H. Fujii, *Science* **1998,** *280*, 560-564.
13. Y. Y. Liu, K. Murata, M. Inaba, I. Takahara, K. Okabe, *Fuel* **2013,** *104,* 62-69.
14. H. T. Luk, C. Mondelli, D. C. Ferre, J. A. Stewart, J. Perez-Ramirez, *Chem. Soc. Rev.* **2017,** *46,* 1358-1426.
15. J. Gong, H. Yue, Y. Zhao, S. Zhao, L. Zhao, J. Lv, S. Wang, X. Ma, *J. Am. Chem. Soc.* **2012**, *134*, 13922-13925.
16. M. H. Baik, M. Newcomb, R. A. Friesner, S. J. Lippard, *Chem. Rev.* **2003,** *103*, 2385-2419.
17. R. Balasubramanian, S. M. Smith, S. Rawat, L. A. Yatsunyk, T. L. Stemmler, A. C. Rosenzweig, *Nature* **2010,** *465*, 115-131.
18. R. Raja, P. Ratnasamy, *Appl. Catal. A-Gen.* **1997,** *158*, L7-L15.
19. E. V. Kudrik, P. Afanasiev, D. Bouchu, J. M. M. Millet, A. B. Sorokin, *J. Porphyr. Phthalocyanines* **2008,** *12*, 1078-1089.
20. A. B. Sorokin, E. V. Kudrik, D. Bouchu, *Chem. Commun.*, **2008,** 2562-2564.
21. J. S. Woertink, P. J. Smeets, M. H. Groothaert, M. A. Vance, B. F. Sels, R. A. Schoonheydt, E. I. Solomon, *Proc. Natl. Acad. Sci. U. S. A.* **2009,** 106, 18908-18913.
22. M. J. Wulfers, S. Teketel, B. Ipek, R. F. Lobo, *Chem. Commun.* **2015,** *51*, 4447-4450.
23. E. V. Starokon, M. V. Parfenov, S. S. Arzumanov, L. V. Pirutko, A. G. Stepanov, G. I. Panov, *J. Catal* **2013,** *300,* 47-54.
24. M. H. Groothaert, P. J. Smeets, B. F. Sels, P. A. Jacobs, R. A. Schoonheydt, *J. Am. Chem. Soc.* **2005,** *127,* 1394-1395.
25. S. Grundner, M. A. C. Markovits, G. Li, M. Tromp, E. A. Pidko, E. J. M. Hensen, A. Jentys, M. Sanchez-Sanchez, J. A. Lercher, *Nat. Commun.* **2015,** *6*, 7546.
26. K. Narsimhan, K. Iyoki, K. Dinh, Y. Roman-Leshkov, *ACS Central Sci.* **2015,** *2,* 424-429.
27. G. I. Panov, A. K. Uriarte, M. A. Rodkin, V. I. Sobolev, *Catal. Today* **1998,** *41*, 365-385.
28. G. I. Panov, V. I. Sobolev, K. A. Dubkov, V. N. Parmon, N. S. Ovanesyan, A. E. Shilov, A. A. Shteinman, *React. Kinet. Catal. Lett.* **1997,** *61*, 251-258.
29. C. Coperet, *Chem. Rev.* **2010,** *110,* 656-680.
30. J. Joubert, A. Salameh, V. Krakoviack, F. Delbecq, P. Sautet, C. Coperet, J. M. Basset, *J. Phys. Chem. B* **2006,** *110*, 23944-23950.
31. S. M. Schimming, G. S. Foo, O. D. LaMont, A. K. Rogers, M. M. Yung, A. D. D'Amico, C. Sievers, *J. Catal.* **2015,** *329*, 335-347.
32. S. M. Schimming, O. D. LaMont, M. Konig, A. K. Rogers, A. D. D'Amico, M. M. Yung, C. Sievers, *ChemSusChem* **2015,** *8*, 2073-2083.
33. N. B. Colthup, L. H. Daly, S. E. Wiberley, *Introduction to Infrared and Raman spectroscopy*, **1990** p. 51.
34. Q. Fu, H. Saltsburg, M. Flytzani-Stephanopoulos, *Science* **2003,** *301*, 935-938.
35. G. Jacobs, P. M. Patterson, L. Williams, E. Chenu, D. Sparks, G. Thomas, B. H. Davis, *Appl. Catal. A-Gen.* **2004,** *262*, 177-187.
36. C. Binet, A. Badri, J. C. Lavalley, *J. Phys. Chem.* **1994,** *98*, 6392-6398.
37. C. Descorme, Y. Madier, D. Duprez, *J. Catal.* **2000,** *196*, 167-173.
38. F. De Smet, P. Ruiz, B. Delmon, M. Devillers, *J. Phys. Chem. B* **2001,** *105*, 12355-12363.
39. Z. G. Yan, S. L. T. Andersson, *J. Catal*. **1991,** *131*, 350-368.
40. B. Monnerat, L. Kiwi-Minsker, A. Renken, *Chem. Eng. Sci.* **2001,** *56*, 633-639.
41. T. Sperle, D. Chen, R. Lodeng, A. Holmen, *Appl. Catal. A-Gen.* **2005,** *282*, 195-204.

10.1002/anie.201704704

WILEY-VCH

COMMUNICATION

Methanol and ethanol are produced continuously from methane and oxygen in a single reaction over a catalyst consisting of NiO clusters on ceria-zirconia. Oxygen is used as an abundantly available oxidant for this reaction and the presence of steam ensures the production of alcohols as opposed to products of complete combustion of methane.

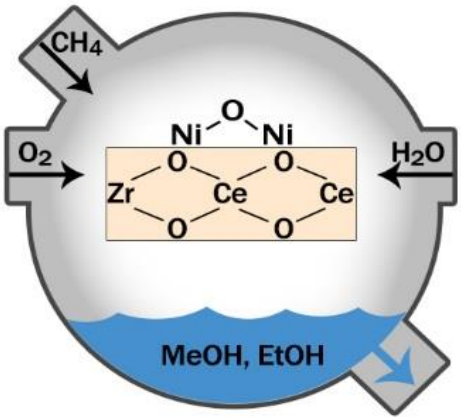

*C. Okolie, Y. F. Belhseine, Y. Lyu, M.M. Yung, M.H. Engelhard, L. Kovarik, E. Stavitski, C. Sievers**

Page No. – Page No.

Conversion of Methane to Methanol and Ethanol over Nickel Oxide on Ceria-Zirconia in a Single Reactor